형상기억합금을 이용한 고속도로 강교량의 면진

Seismic base isolation for highway steel bridges using shape memory alloys

최 은 수[1]   ·   전 준 창[2]

Choi, Eun Soo   *Jeon, Jun Chang*

요   약 : 기존교량의 내진성능개선 및 신설교량의 지진보호에 납-고무 베어링은 좋은 효과를 보여주고 있다. 그러나 납-고무 베어링은 사용상에 있어 문제점이 있으며, 이를 개선하기 위하여 형상기억합금(shape memory alloy)을 이용한 면진장치를 본 연구에서 제시하였다. 3경간 연속 고속도로 강교량의 지진해석을 통하여 납-고무베어링과 고무베어링 및 형상기억합금 와이어와의 조합 면진장치의 지진거동을 비교하였다. 해석결과 형상기억합금 와이어+고무베어링 시스템이 납-고무베어링과 거의 유사한 거동을 보여주었으며, 특히 제시된 면진장치는 상대변위의 제어 및 잔류변형에 있어 기존의 납-고무 베어링에 비해 성능이 우수했다.

AABSTRACT : Conventional lead-rubber bearings may be unstable in case of strong ground motions. To address this problem, this paper proposed a new concept of isolation device wherein shape memory alloy wires were incorporated in an elastomeric bearing. A three-span continuous steel bridge was used for seismic analyses to compare the performance of lead-rubber and proposed bearings. The proposed bearings showed almost the same performance as the lead-rubber bearings. In particular, the proposed bearings limited relative displacement effectively with strong ground motions and recovered its near original undeformed shape.

핵 심 용 어 : 형상기억합금, 납-고무 베어링, 교량 내진해석, 면진장치

KEYWORDS : shape memory alloy, lead-rubber bearings, seismic bridge analysis, isolation device

1. Introduction

Base isolation, in recent years, is a general concept to protect bridges from seismic hazards. Kelly(1986) provided historical reviews and a recent literature on isolation systems. Various isolation devices have been proposed and several concepts have been merged into the seismic isolation bridges.

One of the most popular isolation device is a lead-rubber bearing. Since the lead-rubber bearing was developed in 1975 (Skinner et. al. 1975), they have been being used for new constructions as well as a retrofit measure to mitigate earthquake hazards for bridges. They have a large energy dissipation capacity due to the hysteresis of the plastic deformation of a lead-core compared with elastomeric bearings, thus the bearings can reduce the relative displacement between decks and piers. However, the bearings have problems such as 1) instability due to large deformation and 2) unrecovered residual deformation after a strong earthquake and thus an additional device is required to restraint large deck displacement.

Shape memory alloy (SMA) is considered as a alternative to solve these problems. The SMA acts as both dampers and restrainers due to its special behavior of superelasticity. A SMA shows a thermoplastic martensitic phase transformation. When the SMA cooled under its transformation temperature, its current state (austenite) shifts to the lower temperature martensite state. This transformation is also observed with stressing the

material. The stress-induced martensite (SIM) is unstable thermally. Therefore, the material can recover its strain and go back to austenite state as soon as the stress is released; which is referred to as superelasticity. The superelasticity of a SMA occurs only when the alloy is stressed beyond the transformation temperature range, in other words, above the austenite finish temperature. Laying aside the superelasticity, various hysteretic shapes through material selection and various heat treatment, large ductility and excellent endurance against fatigue of SMAs let them a alternative material for seismic protection systems.

Grasser and Cozzarelli (1991) suggested the use of Nitinol (Ni-Ti alloy) SMA as a seismic damper. They established one-dimensional constitutive model for superelastic behavior and verified the model with experimental work. Dolce et al. (2000) developed a seismic damper using SMA wires. The effectiveness of the damper was proved through experimental works.

DesRoches and Delemont (2002) used SMA bars instead of steel cable restrainers in a multiple span simply supported bridge with elastomeric bearings in longitudinal direction. They showed that the SMA bars are more effective to restraint relative deck displacement than the conventional steel cable restrainers. Wilde et al. (2000) also used SMA bars combining with elastomeric bearings for bridges in transverse direction. The SMA system was verified as an effective device to control relative deck displacement.

The bar type of SMAs was used in the above two applications of SMAs for bridges and the bars installed outside elastomeric bearings. Therefore, an additional work is required to install the SMA bars. Furthermore, a device is required to prevent a buckling problem that may occur when the SMA bar is compressed.

This study proposed the combined isolation device of an elastomeric bearings and SMA wires in a body. The proposed device can provide a damper with the desired properties of the alloy. Furthermore, the device has an inherent centering ability due to

superelastic behavior and a capacity to restrict displacement due to the hardening effect of the SIM.

In this paper, the proposed device will be investigated on the effectiveness for protecting bridges from seismic loads using El Centro ground record scaled to different magnitudes. The performance of the device is presented together with that of a conventional isolation system of lead-rubber bearings.

2. Shape memory alloy

"Shape memory" means the ability of recovering large strains induced for certain alloys (Ni-Ti, Cu-Al, etc) spontaneously or by heating, without any residual deformation. The particular characteristics of shape memory alloys is strongly related to a reversible solid-solid phase transformation, which can be thermal or stress-induced.

A SMA remains in the austenite state at relatively high temperatures, while it changes to the martensite state with cooling. In the stress-free state a SMA has four states according to temperature variation: M_s and M_f during cooling, A_s and A_f during heating. M_s and M_f illustrate the temperature at which the transformation starts and finishes, respectively. A_s and A_f indicate that at which the inverse transformation starts and finishes, respectively.

For some SMAs, such as Nitinol (NiTi SMA), the phase transformation can be induced by a stress at room temperature if the alloys have the appropriate formulation and treatment. When a SMA in austenite state is stressed, a phase change from austenite to martensite occurs at a critical stress level because the martensite state becomes stable over the critical stress value. In reversely unloading process, since unstressed martensite is unstable, the austenite state again becomes stable and the original undeformed shape is recovered.

Nitinol shape memory alloys (NiTi SMAs) hold several desirable properties for using as dampers and restrainers in bridges. These properties are: (1) large elastic strain range; (2) hysteretic damping; (3)

highly reliable energy dissipation due to repeatable solid state phase transformation; (4) strain hardening at strains above 6%; (5) excellent fatigue resistance; and (6) excellent corrosion resistance. Looking at the stress-strain relationship of SMAs in Fig. 1, their primary futures of the superelastic effects can be understood. NiTi SMAs, at first, show elastic range, then a long horizontal plateau, followed by a significant stiffness hardening and, in unloading process, a large hysteretic area is developed without any residual strain.
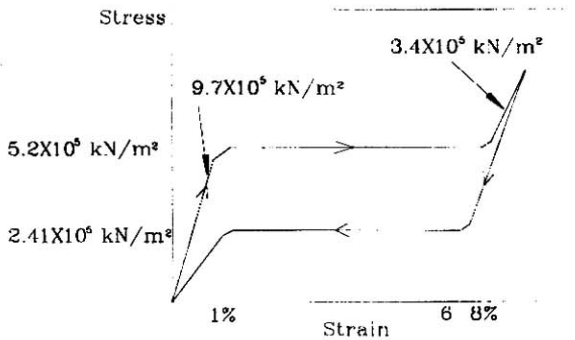

Fig. 1. Idealized stress-strain relationship for superelastic shape memory alloy

This future possesses a high level of energy dissipation and the stress-induced martensite state, occurring approximately at 6-8% strain, is very useful as for restrainer action.

3. SMA-rubber bearing

A SMA-rubber bearing is composed of an conventional elastomeric bearing and SMA wires which wrap the bearing in longitudinal direction. However, since the initial large stiffness and yield strength of the SMA can transfer large inertia forces from decks to piers, the initial elastic range should be removed to use the SMA wire as a damper incorporated with an elastomeric bearing. As shown in Fig. 2, the pre-strain SMA wire shows almost rigid-plastic behavior like a lead-core in a lead-rubber bearing. If an elastomeric bearing is winded

by the pre-strain SMA wire in longitudinal direction as shown in Fig. 3(a), a SMA-rubber bearing is completed. Even when the elastomeric bearing is moving in left or right side, the pre-strain SMA wire is always in tension state. Therefore, the hysteretic curves of the pre-strain SMA wire shown in Fig. 3(a) are developed not in tension but also in compression, antisymmetrically.
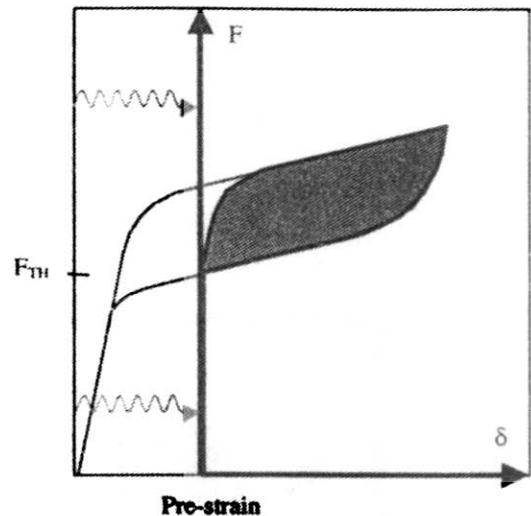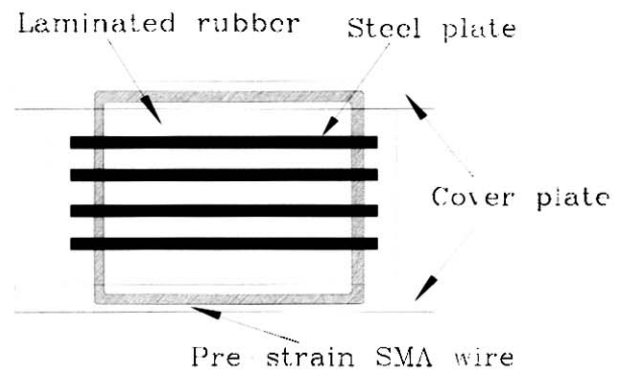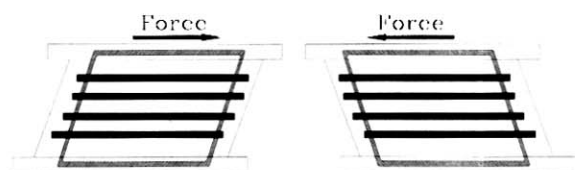

Fig. 2. Effects of pre-strain SMA

(a) Elevation view of a SMA-rubber bearing

(b) Deformed shape of a SMA-rubber bearing

Fig. 3. SMA-rubber bearing and its deformation

4. Analytical models of lead-rubber bearing & SMA-rubber bearing

The lead-rubber bearing (LRB) and the SMA-rubber bearing (SRB) used in this study has the same elastomeric bearing (EB) with 457mm x 305mm x 152mm (LxWxH). The elastomeric bearing can be modeled with bilinear behavior whose properties are: (1) initial stiffness = 1.576 kN/mm; (2) post yield stiffness =0.525 kN/mm; and yield force =24.02 kN.

The lead-rubber bearing has a lead-core of 63.5 mm at the center of the elastomeric bearing. The LRB is also modeled with bilinear of the properties: (1) initial stiffness = 4.203 kN/mm; (2) post yield stiffness = 0.42 kN/mm; and (3) yield force =42.70 kN. The above two models for the both bearings is based on Kelly's study (1997) and Choi's study (2002).

The SMA wire in this study is designed to have the same yield force as the difference between the yield forces of the LRB and the EB. Therefore, as shown in Fig. 4, the yield force of the SMA wire is equal to 18.68 kN. The loading yield strength is assumed to be 410 N/mm^2 and the unloading one is 140 N/mm^2 based on DesRoches's study (2002). Thus, the required yield strength of the pre-strain SMA wire in

Fig. 3(a) is 270 N/mm^2 and the required area is 69.2 mm^2. It is assumed that the yield occurs at 1% strain and the martensite phase transformation develops at 6% strain. The SMA wire of 2.03 m is applied and, for the case, the yielding starts at 20.3 mm and the martensite phase transformation occurs at 122 mm deformation. The initial stiffness (K_1) is 9.2 kN/mm and the hardening ratios for post yield and martensite state transformation are 0.01 and 0.45, respectively, which depends on the components' ratio in the alloy. The SMA wire is designed to be reached at the 6% strain when the elastomeric bearing has 0.8 of its 100% shear deformation (152 mm).
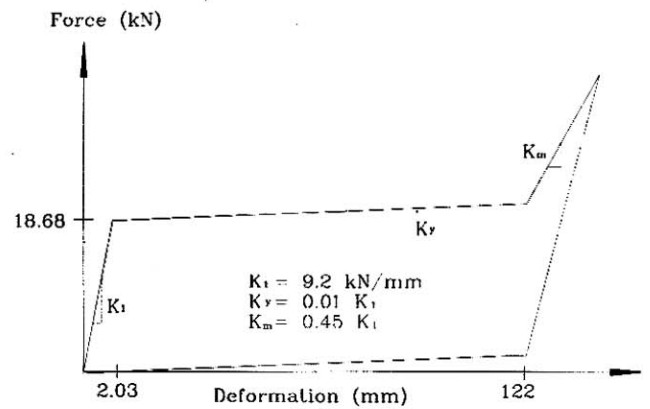

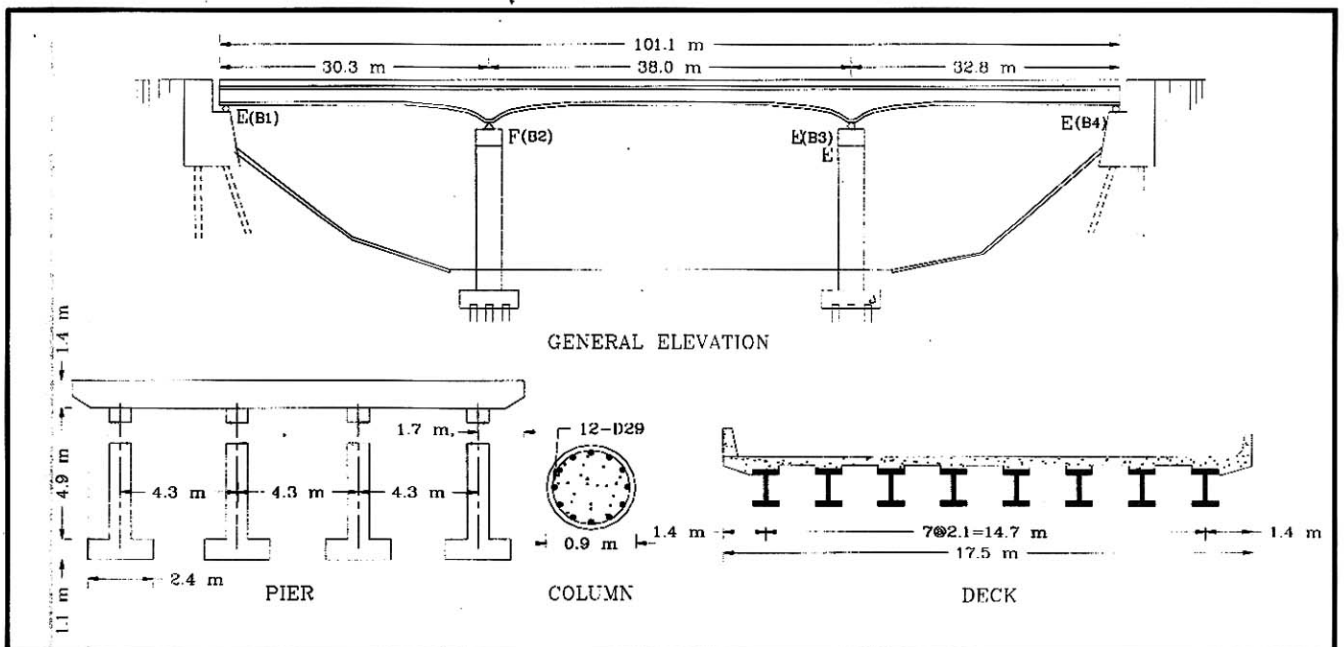Fig. 4. Property of pre-strain SMA wire

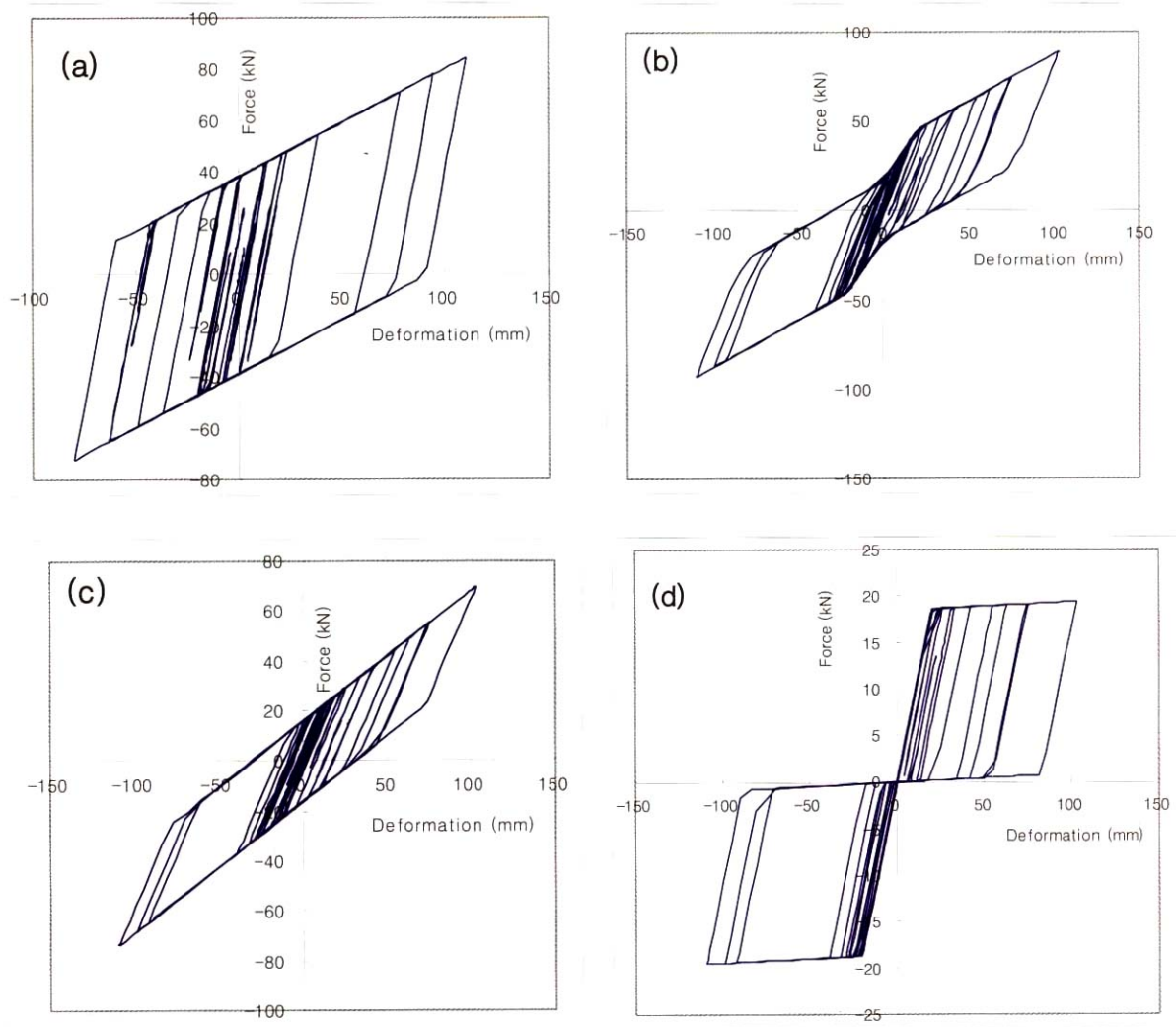Fig. 5. Layout of a continuous multi-span steel bridge

Fig. 6. Hysteresis curves of (a) LRB, (b) SRB (joint of SMA wire and elastomeric bearing),
(c) elastomeric bearing and, (d) SMA wire for the ground motion of 0.8g PGA.

5. Analytical modeling of the continuous steel bridge

A three-span continuous steel bridge as shown in Fig. 5 is modeled for this study. Originally, the bridge has an array of fixed steel bearings on the first pier from left and expansion steel bearings on the other locations. These steel bearings are replaced by lead-rubber bearings or SMA-rubber bearings.

The bridges consist of several components such as columns, abutments, steel bearings, foundations with piles, and superstructures; some of them, particularly columns, exhibit highly nonlinear behavior. Therefore,

two-dimensional nonlinear analytical model of the bridge in longitudinal direction is developed using DRAIN-2DX nonlinear analysis program (Prakash et al., 1992). The superstructure is usually expected to remain linear under longitudinal earthquake motions so that it is modeled using a linear element. In the bridge model, abutments are ignored since they can influence the performance of the both type of bearings due to pounding between decks and abutments. Columns consist of 22 fiber elements for unconfined and confined concrete and reinforcements. The pile foundations are modeled as a fixed condition.
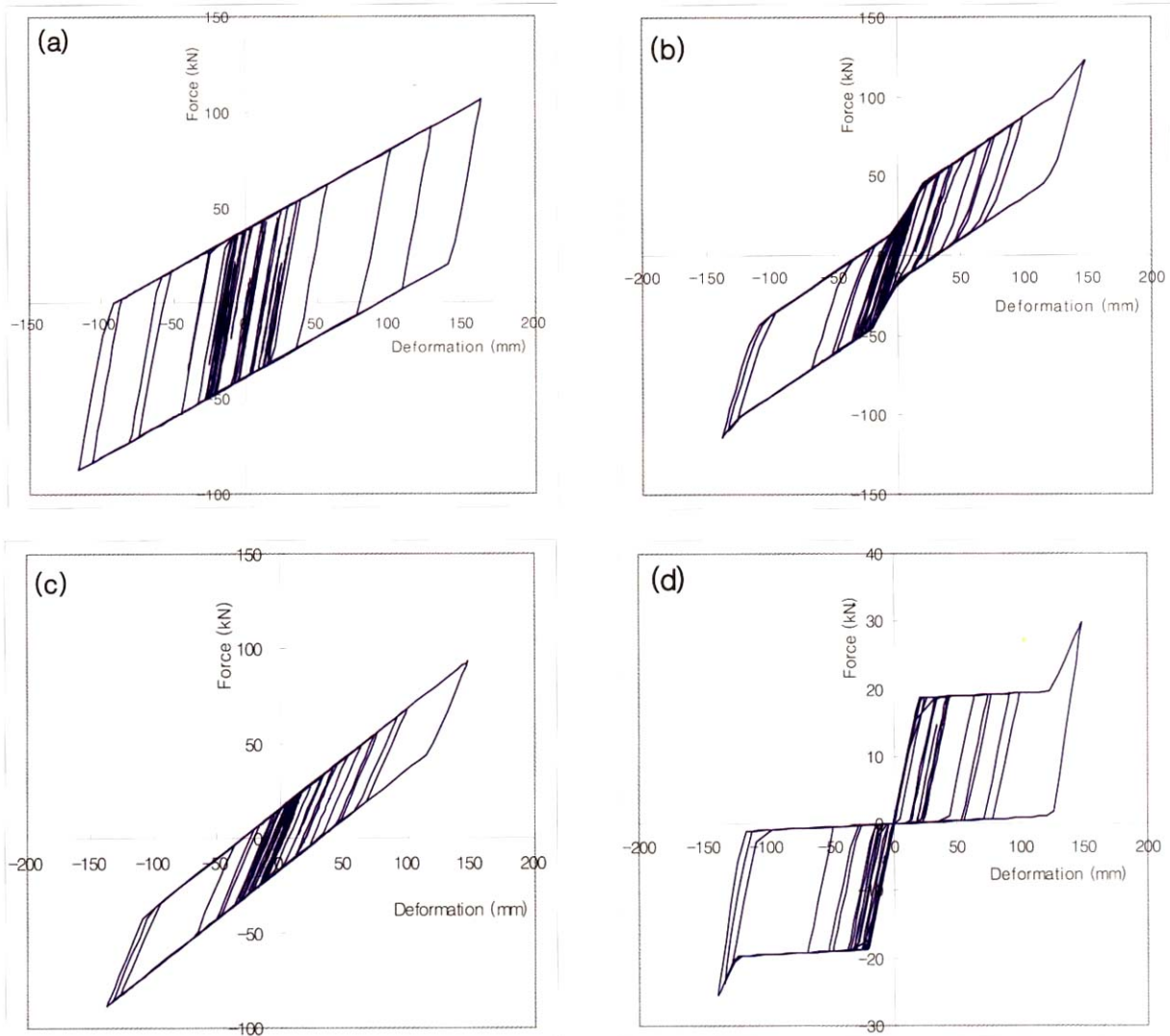
Fig. 7. Hysteresis curves of (a) LRB, (b) SRB (joint of SMA wire and elastomeric bearing),
(c) elastomeric bearing and (d) SMA wire for the ground motion of 1.0g PGA.

6. Results

To evaluate the effectiveness of the proposed SMA-rubber bearings by comparing with conventional lead-rubber bearings for mitigating seismic hazards, the original El Centro ground record (PGA=0.348 g) is scaled from weak to strong, such as 0.2, 0.4, 0.6, 0.8 and 1.0 g, and applied for the seismic analysis of the example bridge shown in Fig. 5. The interesting responses are deck displacement, relative displace -ment between deck and pier, pier drift ratio and residual deformation after earthquake motions.

Besides, the force developed in the two types of bearings are calculated. The maximum responses for each ground motion intensity are illustrated in Table 1 in which the deck displacement and the relative displacement are equal to the bearing deformation on abutments and piers, respectively. A pier drift ratio is a per cent of a pier top displacement to the pier length.

In the table, the values in parentheses show the per cent of the difference between the responses of the LRB and the SRB bridge to those of the LRB bridge.

Figs. 6 and 7 show the hysteresis curves of the three components of LRB, EB, and SMA wire and the joint hysteresis of EB and SMA wire on the first pier in Fig. 5 for the ground records of 0.8 g and 1.0 g PGA, respectively.

As expected, the analytical model of a SMA wire in Fig. 6(d) shows the same hysteresis curve in tension and compression antisymmetrically.

In Figs. 6(a) and (b), the maximum developed forces are 85.3 kN at 112 mm and 92.4 kN at 108 mm for the LRB and the SRB, respectively. In Fig. 7, the hardening effect due to the SIM, which begins at the deformation of 122 mm, is activated and the maximum force of the SBR is 120.9 kN at 145 mm. When the hardening due to stress-induced martensite occurs, the large force in the SRB is developed and its deformation is restricted.

6.1 Deck Displacement

For deck displacement, the bridge with the SBR has larger deck displacements for weak and moderate ground motions of 0.2, 0.4 and 0.6 g PGA by 16-40% than the bridge with the LRB does. However, the SRB bridge's deck displacements are smaller by 2-5% with strong ground motions of 0.8 and 1.0 g PGA than the LRB bridges's deck displacements. The reason of this situation is due to the hardening by the SIM. For the 0.8 g PGA ground motion, the SRBs on piers are not activated with the hardening as shown

in Fig. 6, but the hardening occurs in the SRBs on abutments whose deformations are larger than the hardening initiated deformation of 122 mm as illustrated Table 1. For the 1.0 g PGA ground motion, the SRBs on both piers and abutments are activated with the hardening since the deformations of the bearings are larger than the deformation of 122 mm as shown in Table 1. Therefore, the hardening effect by the SIM in the SRB obtains a desirable result to restrict the deck displacement with strong ground motions.

Looking at the result for 0.2 g PGA ground motion in Table 1, the force developed in a SRB is smaller than that in a LRB, however, the deck displacement with the SRB is larger than that with the LRB. This happens due to the energy dissipation capacity of the two bearings. The LRB designed in this study has larger energy dissipation capacity than the SRB, which can be explained through comparing the graphs of (a) and (b) in Fig. 6, therefore the LRB can restrict the deck displacement effectively even with the larger bearing force for weak and moderate ground motions.

The deck displacement consists of column's and bearing's deformation. Thus, the critical factors for generating deck displacement are the forces developed in bearings and the amount of energy dissipation. The former controls the column's deformation and the latter does the bearing's deformation. In general, the developed forces in the SRBs are larger than those in

Table 1. Maximum values of interesting responses for LRB and SRB bridge

PGA	LRB bridge					SRB bridge				
	Deck displ. (mm)	Relative displ. (mm)	Residual deform. (mm)	Pier drift (%)	Force in bearing (kN)	Deck displ. (mm)	Relative displ. (mm)	Residual deform. (mm)	Pier drift (%)	Force in bearing (kN)
0.2	27.7	11.0	2.5	0.25	43.0	38.6 (39.4%)	18.3 (66.4%)	0.0	0.31 (24.0%)	42.4 (-1.3%)
0.4	57.8	32.1	7.1	0.40	51.9	77.2 (33.6%)	47.0 (46.4%)	0.0	0.44 (10.0%)	59.6 (14.8%)
0.6	98.6	64.3	2.3	0.49	65.5	114.3 (15.9%)	78.0 (21.3%)	0.0	0.55 (12.2%)	76.1 (16.2%)
0.8	154.6	111.6	11.9	0.62	85.3	151.6 (-1.9%)	108.3 (-3.0%)	0.0	0.65 (4.8%)	92.4 (8.3%)
1.0	213.9	161.4	20.0	0.76	106	202.8 (-5.2%)	145.3 (-10.0%)	0.0	0.86 (13.2%)	120.9 (14.1%)

the LRBs, however the SRBs have smaller energy dissipation than the LRBs as shown in Figs. 6 and 7.

6.2 Relative Displacement

The relative displacements between deck and pier with the SRBs are smaller for the strong ground motions than that with the LRBs.

The cause of this phenomenon is identical with that for the deck displacement.

The SRBs have 0.60 kN/mm post yield stiffness and do the LRBs 0.42 kN/mm from the chapter 4. The SRBs generate the larger relative displacement even with the larger hardening stiffness since the bearings have smaller damping comparing with the LRBs before the stiffness hardening by the SIM occurs.

6.3 Pier Drift

The pier drift ratios with the SRB for all ground motions are larger by 5-24% than those with the LRB. Although the deck displacement and the relative displacement with the SRB are smaller for the strong ground motions than those with the LRB, the SRBs for the same ground motions produce larger pier drift ratios than the LRBs. The hardening by the SIM phase transformation transfers a large force to the pier and thus the pier drift becomes large. The smallest difference in the pier drift ratio occurs with

the 0.8 g PGA ground motion in which the SRBs on the pier are fully deformed without the hardening by the SIM.

The two factors to influence pier drifts are energy dissipation by the bearings and the forces developed in the bearings.

The pier drifts decrease with increasing energy dissipation but increase with increasing the bearing forces. Therefore, due to the small damping and the large bearing forces, the SRBs always produce larger pier drift than the LRBs. When the stiffness hardening by the SIM is induced, it increases the pier drift more.

Finally, the pier drift ratio of the both bridges even with the strongest ground record is less than 1.0 at which a minor damage starts in piers (Lam, 1994). Therefore, the both types of isolation bearings protect piers satisfactory.

6.4 Residual Deformation

The LRBs remain residual deformation even with the weakest ground motion. However, the SRBs recover almost all deformation to original location. Fig. 8 shows the time histories of the LRBs' and the SRBs' deformation with 0.8 g PGA ground motion. The LRBs remains almost constant deformation of 11.9 mm after 28.0 second. The SRBs can recover all deformation even when they experienced the hardening by the stress-induced martensite.
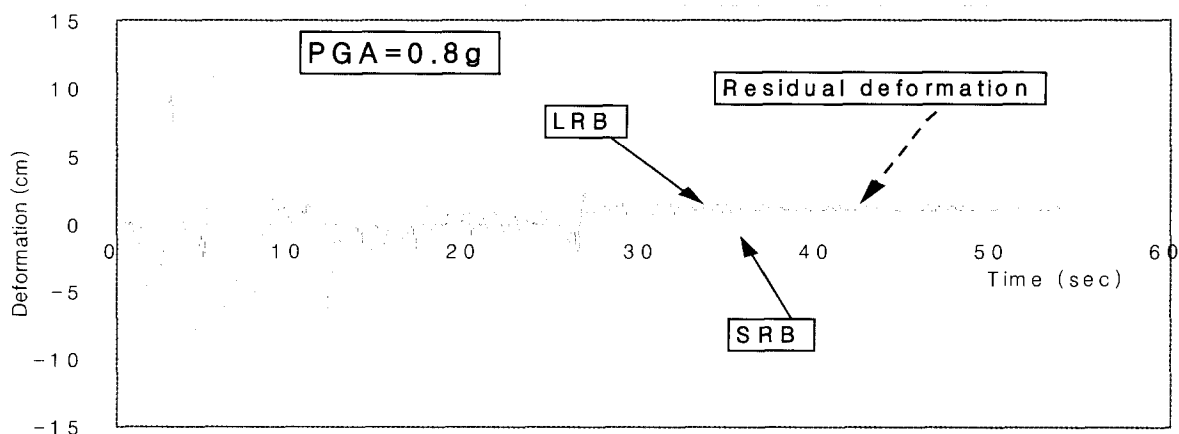

Fig. 8. Time histories for LRB's and SRB's deformation with 0.8g PGA ground motion and residual deformation

A residual deformation of the bearings after an earthquake makes it difficult to repair the damages on piers and else where since it is required to place the deck to the original location.

7. Conclusions

This paper proposed a new concept for incorporating SMA wires into an elastomeric bearing in a body and showed the performance of the bearings compared with that of conventional lead-rubber bearings. A three-span continuous steel highway bridge was used for the seismic analysis.

The SMA-rubber bearings restrained the deck displacement and the relative displacement between deck and pier satisfactory with strong ground motions. Although they increase pier demand a little compared with lead-rubber bearings, they protect piers safely from strong earthquakes.

A variable characteristics of the SMA-rubber bearings do not remain any residual deformation even after strong ground motions. However, conventional lead-rubber bearings exposed to strong earthquakes have to be replaced because of residual deformation.

In construction site, the proposed SMA-rubber bearings do not require any additional work to install them since the SMA wire is unified into an elastomeric bearing in a body.

Acknowledgement

Reference

Choi, E. (2002), Seismic Analysis and Retrofit of Mid-America Bridges, Dept. Civil and Environmental Engr. Georgia Institute of Technology, Atlanta, Georgia, USA.

DesRoches, R. and Delemont, M. (2002), Seismic retrofit of simply supported bridges using shape memory alloys, Engineering Structures, 2002;24; 325-332.

Dolce, M., Cardone, D., and Marnetto, R. (2000), Implementation and testing of passive control devices based on shape memory alloys, Earthquake Engineering and Structure Dynamics, 2000;29;945-968.

Grasser E.J. and Cozzarelli F.A. (1991), Shape memory alloys as new materials for aseismic isolation, Journal of Engineering Mechanics, ASCE, 117(11): 2590-608.

Kelly, J. M. (1997), Earthquake- Resistance Design with Rubber, Springer, London, 1997, 2nd.

Kelly, J.M. (1986), A seismic base isolation: a review and bibliography, Soil Dynamics and Earthquake Engineering, 1986;5;202-16.

Lam, I. P. (1994), Soil-Structure Interaction Related to Piles and Footings, Proceedings of the Second International Workshop on the Seismic Design of Bridges, Queenstown, News Zealand.

Skinner, R. I., Robinson, W.H., and McVerry, G. H. (1993), An Introduction to Seismic Isolation, JOHN WILEY & SONS, New York.

Wilde, K., Gardoni, P. and Fujino, Y. (2000), Base isolation system with shape memory alloy device for elevated highway bridges, Engineering structures, 2000;22;222-229.